

# Hit Rate of Space Weather Forecasts of the Japanese Forecast Center and Analysis of Problematic Events on the Forecasts between June 2014 and March 2015

S. Watari, H. Kato, and K. Yamamoto

National Institute of Information and Communications Technology, Tokyo, Japan

E mail (watari@nict.go.jp).

Accepted: 18 September 2015

**Abstract** The hit rate of space weather forecasts issued by the Japanese forecast center in the National Institute of Information and Communications Technology (NICT) between June 2014 and March 2015 are compared with that by the persistence method. It is shown that the hit rate of the forecasts by the Japanese center is better than that by the persistence method. Several problematic events on the space weather forecasts during the same period are analyzed. Those events are (1) geomagnetic storms associated with coronal mass ejections (CMEs) on 9 September 2014 and on 15 March 2015 with different durations of southward interplanetary magnetic field (IMF), (2) a large active region, AR 12192 without CMEs, solar energetic particle events, and geomagnetic storms, (3) a geomagnetic storm on 7 January 2015 caused by a faint CME, and (4) disagreement between the in-situ observation at 1 AU and the prediction of the Potential Field Source Surface (PFSS) model on timing of sector crossing in January 2015.

© 2015 BBSRSN SWS. All rights reserved

**Keywords:** space weather forecast, solar-terrestrial event analysis workshop, verification, problematic space weather events

## Introduction

The solar-terrestrial environment data analysis workshop, which is called the STE workshop, has been held twice a year in Japan for several decades. This workshop is supported by the Solar-Terrestrial Environment Research Laboratory (STEL), Nagoya University to promote collaborative research activities in Japan. Purpose of this workshop is promoting collaborative analysis of observation and simulation data to study the sun-earth connection events. Three or four scientifically interesting events during the periods are selected for detailed analysis.

In the STE workshop, the result of space weather forecasts issued by the Japanese forecast center in the National Institute of Information and Communications Technology (NICT) are presented to discuss the problematic events on the space weather forecasts during the analysis period for improvement of the forecasts.

Based on the discussion of the STE workshop held with the United Nation Fukuoka Workshop in March 2015, we report the hit rate of the NICT forecasts comparing with that by the persistence method, which uses condition of previous day as today's forecast, and the analysis on several problematic events on the space weather forecasts for the analysis period between June 2014 and March 2015.

## 2. Overview of space weather between June 2014 and March 2015

Sunspot number increased again since the beginning of 2013 and became the maximum value in April 2014 according to the thirteen-month smoothed monthly sunspot number from the Sunspot Index and Long-term Solar Observations, Royal Observatory of

Belgium, Brussels. In October, an active region, AR12192 appeared and produced many M-class and X-class flares. However, this active region did not produce any solar energetic particle events and geomagnetic storms. Geomagnetic activities were still low comparing with recent several cycles.

Table 1 shows solar energetic particle event called 'proton event' which occurred during the analysis period. Enhancements of solar energetic particles greater than 10 MeV were observed several times. However, only one event exceeded proton flux of 10 proton flux unit (pfu).

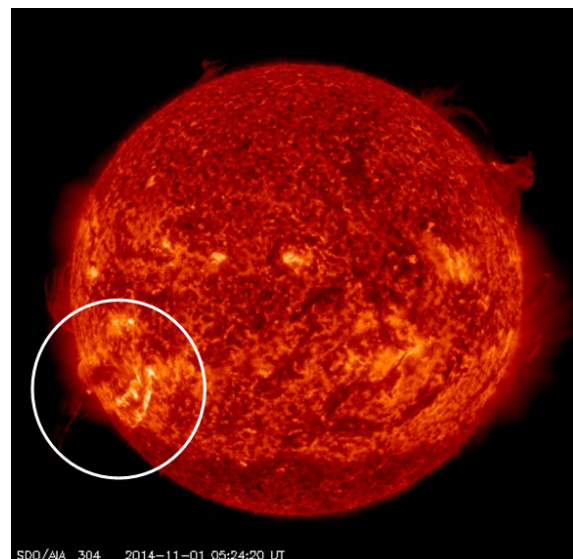


Figure 1. 304 Å image of the Hyder flare (white circle) on November 2014 observed by the SDO/AIA (NASA).

Table 1. Proton event between June 2014 and March 2015

Start time (UT)	End time (UT)	Max. time (UT)	Max. flux (pfu)
2014/09/11 02:55	2014/09/11 23:00	2014/09/12 15:55	126

Table 2. Geomagnetic storms reported by the Kakioka Magnetic Observatory between June 2014 and March 2015

Start time (UT)	End time (UT)	Max. dH at Kakioka (nT)	Min. Dst (nT)	Type
2014/08/27 3.1	2014/08/30 15:00	104	-80	Gradual storm
2014/09/12 15:54	2014/09/13 24:00	109	-75	SC storm
2014/11/04 7.7	2014/11/05 16:00	95	-38	Gradual storm
2014/11/10 02:20	2014/11/10 23:00	72	-57	SC storm
2015/01/07 06:16	2015/01/08 18:00	188	-99	SC storm
2015/03/17 04:45	2015/03/21 15:00	237	-223	SC storm

SC: sudden commencement

Table 3. Definition of forecasts of ISES/UGEOA code

Flare forecast	
Quiet	<50% possibility of C-class flares
Eruptive	C-class flares expected, possibility $\geq 50\%$
Active	M-class flares expected, possibility $\geq 50\%$
Major flares expected	X-class flares expected, possibility $\geq 50\%$
Proton flares expected	proton flares expected, possibility $\geq 50\%$
Warning condition	activity levels expected to increase, but no numeric forecast given
Geomagnetic disturbance forecast	
Quiet	
Active condition expected	$A \geq 20$ or $K=4$
Minor storm expected	$A \geq 30$ or $K=5$
Major magstrom expected	$A \geq 50$ or $K \geq 6$
Severe magstrom expected	$A \geq 100$ or $K \geq 7$
Warning condition	activity levels expected to increase, but no numeric forecast given
Proton forecast	
Quiet	
Proton event expected	10 pfu at $> 10$ MeV
Major proton event expected	100 pfu at $> 100$ MeV
Proton event in progress	$> 10$ MeV
Warning condition	activity levels expected to increase, but no numeric forecast given

Table 2 shows six geomagnetic storms which are reported from the Kakioka Magnetic Observatory, Japan Meteorological Agency (JMA) during the analysis period. One of six storms in Table 2, the November 4, 2015 geomagnetic storm occurred associated with a large filament eruption observed between 4UT and 6UT on 1 November 2014. It is known that geomagnetic storms sometimes occur associated with filament eruptions (Joselyn and McIntosh, 1981). A Hyder flare (Hyder, 1967a and 1967b) was observed associated with this filament eruption. Figure 1 shows the 304 Å image of this event observed by the Solar Dynamics Observatory (SDO)/Atmospheric Imaging Assembly (AIA) (NASA, <http://sdo.gsfc.nasa.gov/>). Enhancement of solar energetic particle flux started several hours after this event.

### 3. Space weather forecasts between June 2014 and March 2015 and their evaluation

The Regional Warning Centers (RWCs) of the International Space Environment Service (ISES) have exchanged their data and information using the URSlgram codes. The UGEOA code is one of the URSlgram codes describing daily forecasts on solar flare activities, geomagnetic disturbances, and occurrence of proton events. Table 3 shows the definition of those forecasts.

(<http://www.spaceweather.org/ISES/code/aaf/ugeoa.html>)

NICT issues forecasts within 24 hours using the ISES/UGEOA code at 6 UT every day (Watari, 2008). Those forecasts during the analysis period are evaluated using the contingency tables. The forecasts of proton events are not evaluated in this study because they are nowcast rather than forecast. We use the flare lists from the National Center of Environment Information (NCEI), National Oceanic and Atmospheric Administration (NOAA) and geomagnetic K indices from the Kakioka Magnetic Observatory, JMA in order to evaluate the forecasts.

Figure 2 shows the monthly occurrence of active days more than or equal to 'eruptive' levels of flare activities (upper panel) and quiet days (the second panel), and monthly hit rates of flare forecasts by the persistence method (the third panel) and monthly hit rates of the NICT forecasts (bottom panel). The average hit rates are 60.5% for the persistence method and 64.7% for the NICT forecasts, respectively.

Figure 3 shows the monthly occurrence of active days more than or equal to 'active' levels of geomagnetic disturbances (upper panel) and quiet days (the second panel), and monthly hit rates of forecasts of geomagnetic disturbances by the persistence method (the third panel) and monthly hit rates of the NICT forecasts (bottom panel). The average hit rates are 66.4% for the persistent method and 72.0% for the NICT forecasts, respectively.

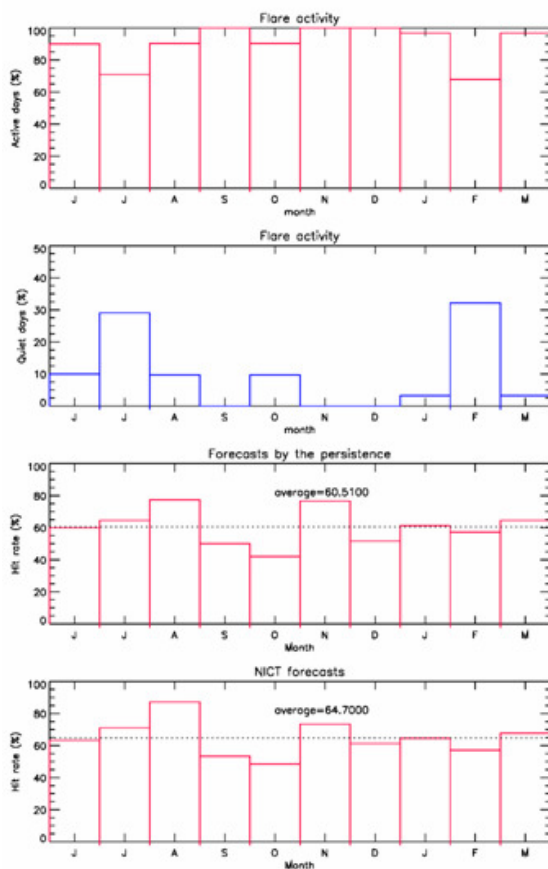


Figure 2. The monthly occurrence of active days more than or equal to 'eruptive' levels of flare activities (upper panel) and quiet days (the second panel), and monthly hit rates of flare forecasts by the persistence method (the third panel) and monthly hit rates of the NICT forecasts (bottom panel).

In this study, the hit rate is defined as the rate of the forecasts which agree with the observed conditions. The hit rates of the forecasts generally exceeded those by the persistence method and appear to be anti-correlated with activities according to those figures.

When we make flare forecasts, we analyze flare history, magnetic classification, and area of each active region. We also refer statistics of flare probabilities based on flare history and magnetic classification and area of each active region. On geomagnetic forecast, we analyze solar sources of geomagnetic storms such as earth-directed halo coronal mass ejections (CMEs) and high-speed solar wind from coronal holes using extreme ultraviolet (EUV) solar images by the SDO/AIA and coronagraph images by the Solar and Hemispheric Observatory (SOHO). We also refer 27-day recurrent geomagnetic activities. These are reason why our forecasts are better than those by the simple persistence method.

#### 4. Problematic case1: Southwards Interplanetary Magnetic Field (IMF) associated with CMEs and their effects

AR12158 produced a M4.5/1N long duration event (LDE) flare with a full halo CME near the center of solar disk at 23:12 UT on September 8, 2014. Enhancement of

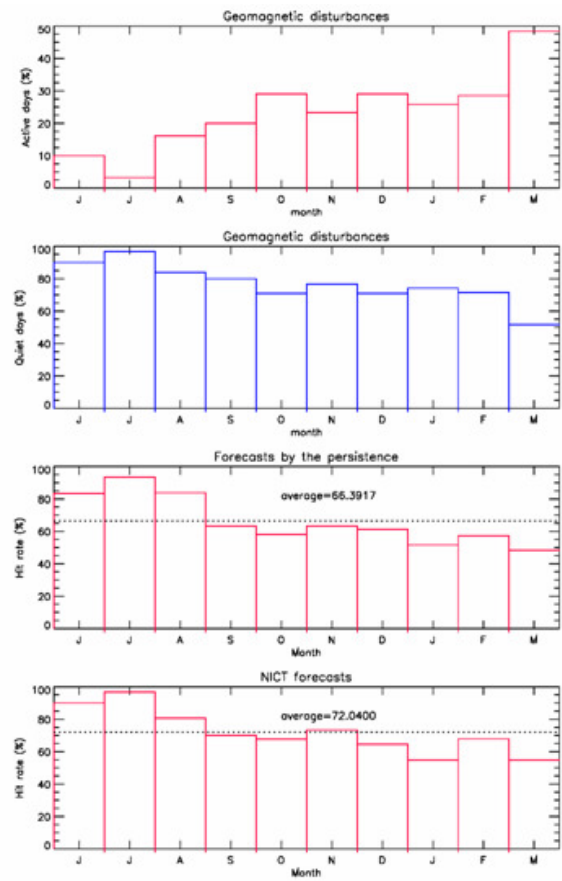


Figure 3. The monthly occurrence of active days more than or equal to 'active' levels of geomagnetic disturbances (upper panel) and quiet days (the second panel), and monthly hit rates of forecasts of geomagnetic disturbances by the persistence method (the third panel) and monthly hit rates of the NICT forecasts (bottom panel).

solar energetic particles by this flare was observed by the GOES satellite. Arrival of an interplanetary shock was observed at 15:54 UT on 12 September at Kakioka as a Sudden Storm Commencement (SSC).

Figure 4 shows one-minute values of solar wind parameters near the earth obtained from the NASA/OMNI data, magnitude of IMF B<sub>1</sub> (the second panel), north-south component of IMF B<sub>z</sub> (the third panel), phi angle of IMF (the forth panel), theta angle of IMF (the fifth panel), speed (the sixth panel), density (the seventh panel), temperature (the eighth panel), and beta (bottom panel) with geomagnetic index, SYM-H (top panel) between 11 and 14. Red line of the eighth panel is temperature calculated from solar wind speed using the empirical equation (Lopez, 1987). It is known that observed temperature often becomes lower than that estimated using solar wind speed in ejecta of coronal mass ejections (CMEs). According to Figure 4, southward IMF of approximately 10 nT continued for approximately two hours associated with the sheath after the shock. Then IMF turned northward and the northward IMF continued for more than two days. As the result, the geomagnetic storm did not grow and magnitude of the geomagnetic storm became relatively small.

Table 4. X-class flares from AR12192 and AR10486

AR12192		AR10486		
Date and time(UT)	Importance	Date and time (UT)	Importance	Comments
2015/10/19 04:17	X1.1	2003/10/23 08:19	X5.4/1B	
2015/10/22 14:02	X1.6/2B	2003/10/23 19:50	X1.1/1N	
2014/10/24 21:07	X3.1/3B	2003/10/26 05:57	X1.2/3B	
2014/10/25 16:55	X1.0/3B	2003/10/28 09:51	X17.2/4B	-full halo CME -proton event -Oct. 29 geomag. storm
2014/10/26 10:04	X2.0/2B	2003/10/29 20:37	X10.0/2B	-full halo CME -proton event -Oct. 30 geomag. storm
2014/10/27 14:12	X2.0/2B	2003/11/02 17:03	X8.3/2B	-full halo CME -proton event -Nov. 4 geomag. storm
-----	-----	2003/11/04 19:29	X28.0/3B	-full halo CME -proton event

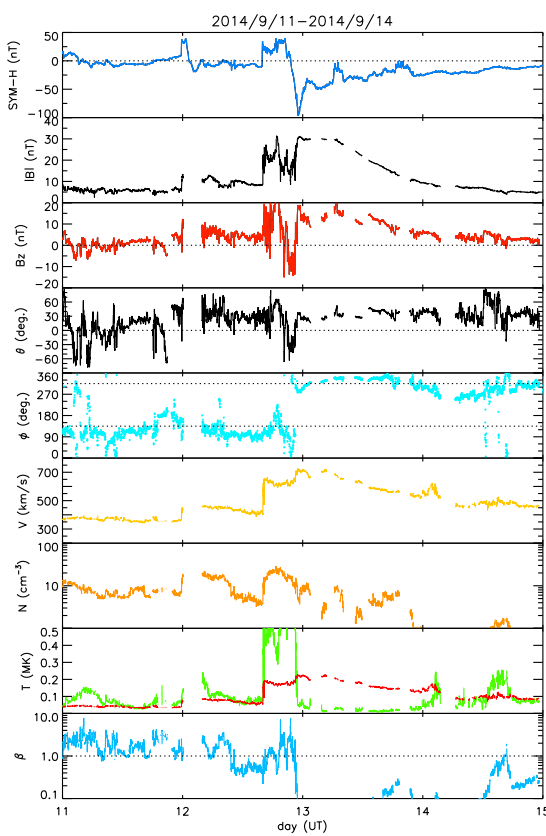


Figure 4. One-minute values of solar wind parameters near the earth (magnitude of IMF  $|B|$ : the second panel, north-south component of IMF  $B_z$ : the third panel, theta angle of IMF: the forth panel, phi angle of IMF: the fifth panel, speed: the sixth panel, density: the seventh panel, temperature: the eighth panel, temperature estimated from speed using the empirical equation: red line of the eighth panel and beta: bottom panel) with geomagnetic index, SYM-H (top panel) between 11 and 14 in September 2014.

This event remarks necessity of a method to investigate southwards IMF associated with the CME based on observation of its solar source. Marubashi (1997) noted a method to investigate orientation of an interplanetary magnetic flux rope associated with a CME using direction of neutral line of solar surface where the CME is initiated. Figure 5 shows the 304 Å

image at the moment of the M4.5/1N flare observed by the SDO/AIA (NASA). Figure 6 shows the synoptic chart of the photospheric magnetic field of Carrington Rotation (CR) 2154 produced by the Wilcox Solar Observatory (WSO). Blue contour lines show the positive regions. The neutral line is black. The arrow in Figure 6 shows the expected orientation of the magnetic flux rope associated with the flare of Figure 5 based on the Marubashi's method (Marubashi, 1997).

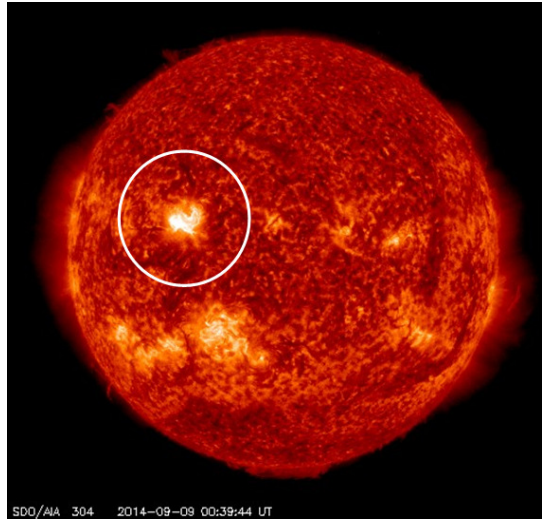


Figure 5. 304 Å image of the M4.5/1N flare (white circle) on 9 September 2014 observed by the SDO/AIA (NASA).

Another event is the March 17, 2015 geomagnetic storm called "St. Patrick event". This geomagnetic storm is caused by the partial halo CME, which occurred around 2 UT on 15 February. This CME was associated with a long-duration C9.1/1F flare (S22W25) at AR12297. Enhancement of solar energetic particles was observed associate with this flare. According to the location of the solar source and the direction of the CME, it was expected that the eastern edge of the CME passed the earth and southward IMF continued for the long time period by the flank passage of the magnetic cloud (see Figure 1(a) in Marubashi and Lepping (2007)).

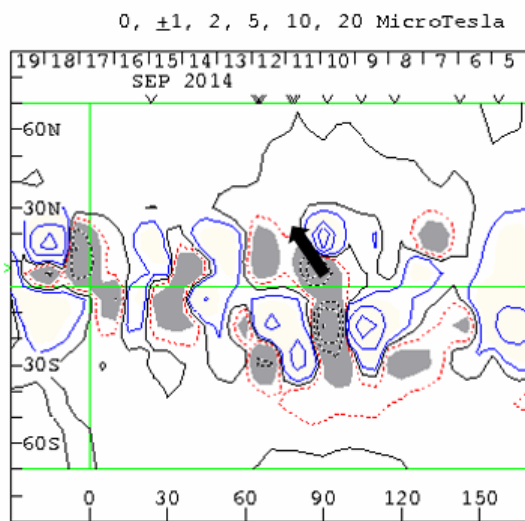


Figure 6. Synoptic chart of the photospheric magnetic field of Carrington Rotation 2154 produced by the WSO. Blue contour lines show the positive regions. The neutral line is black. Arrow shows expected orientation of the magnetic flux rope associated with the CME.

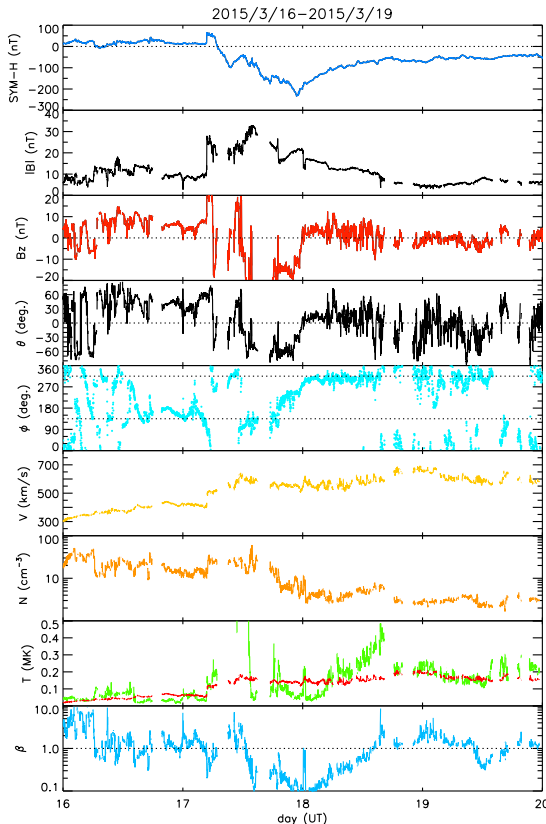


Figure 7. One-minute values of solar wind parameters near the earth with geomagnetic index, SYM-H between 16 and 19 in March 2015. Figure format is same as Figure 4.

Figure 7 is solar wind parameters between 16 and 19. According to Figure 7, southward IMF continued for several hours because a part of the magnetic cloud associated with the CME passed the earth adding to the interplanetary shock and sheath. This event is an

example that long-duration southwards IMF associated with the CME causes an intense geomagnetic storm. Gonzalez, Walter, and Tsurutani (1987) noted that "the interplanetary causes of the intense geomagnetic storms ( $Dst < -100$  nT) are long-duration, large and negative ( $< -10$  nT) IMF  $B_z$  events, associated with interplanetary duskward-electric fields  $> 5$  mV/m, that last for intervals  $> 3$  hours".

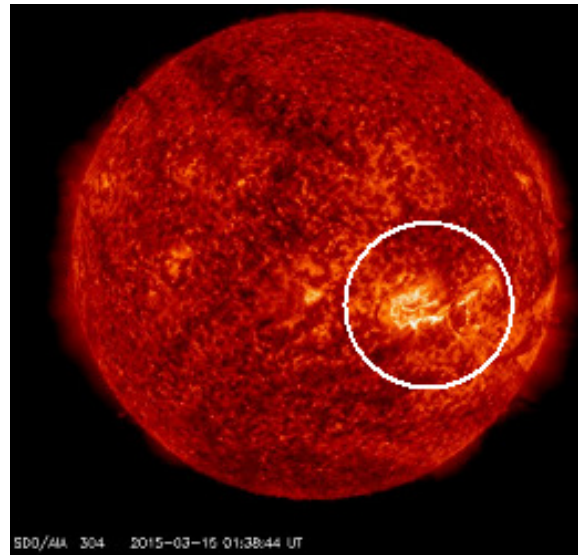


Figure 8. 304 Å image of the C9.1/1F flare (white circle) on 15 March 2015 observed by the SDO/AIA (NASA).

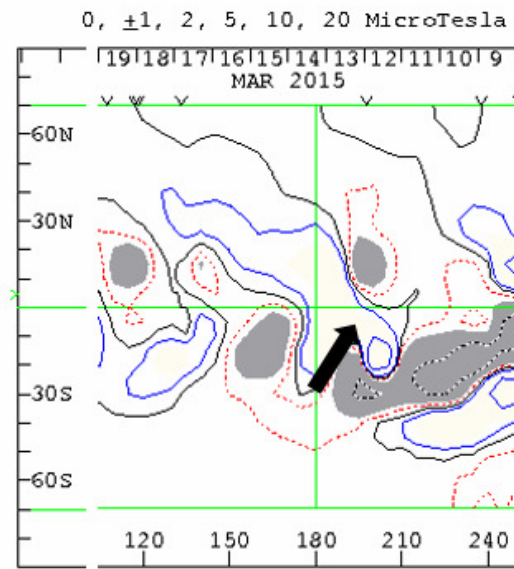


Figure 9. Synoptic chart of the photospheric magnetic field of Carrington Rotation 2161 produced by the WSO. Blue contour lines show the positive regions. The neutral line is black. Arrow shows expected orientation of the magnetic flux rope associated with the CME.

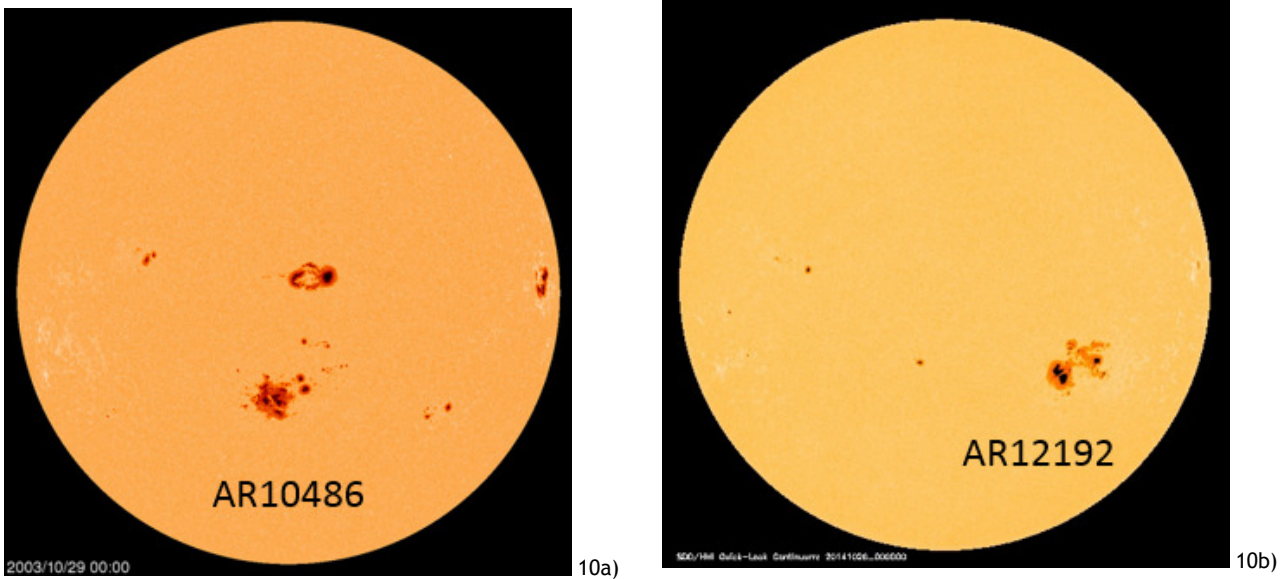


Figure 10. Observations of (a) AR10486 by the SOHO/MDI (ESA&NASA) on 29 October 2003 and (b) AR12192 by the SDO/HMI (NASA) on 26 October 2014.

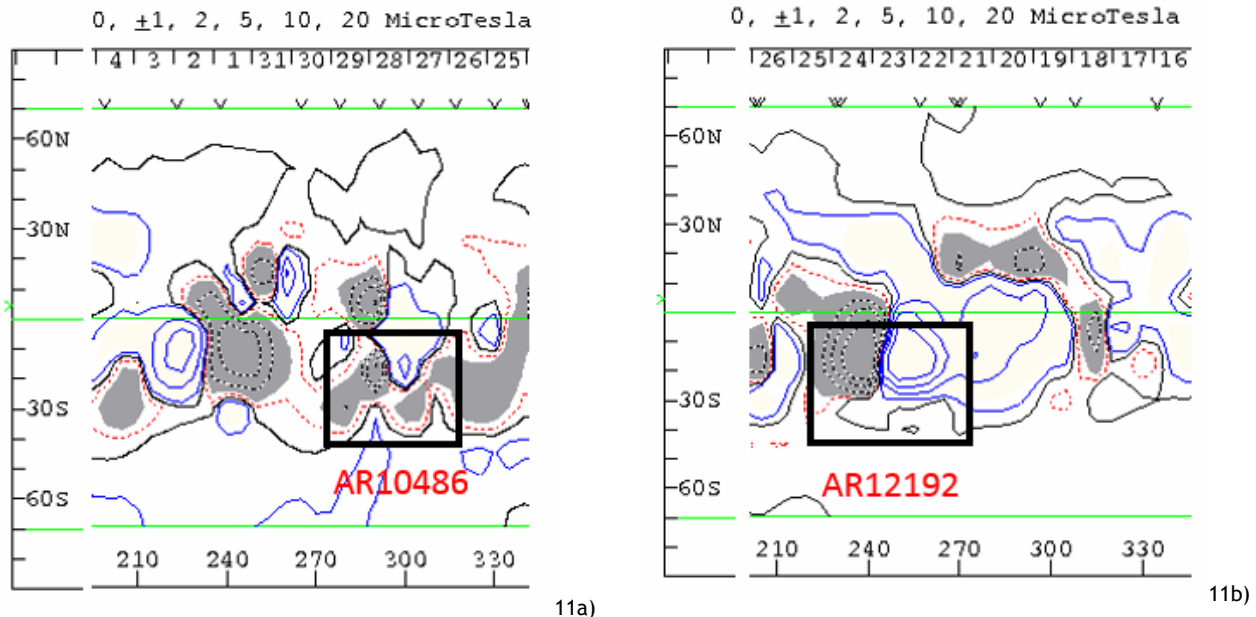


Figure 11 Synoptic charts of the photospheric magnetic field of (a) Carrington Rotation 2009 for AR10486 (left panel) and (b) Carrington Rotation 2156 for AR12192 (right panel) produced by the WSO. Blue contour lines show the positive regions. The neutral line is black.

Figure 8 shows the 304 Å image at the moment of the C9.1/1F flare observed by the SDO/AIA (NASA). Figure 9 shows the synoptic chart of the photospheric magnetic field of CR2161 by the WSO. The arrow shows expected orientation of the magnetic flux rope associated with the flare of Figure 8 based on the Marubashi's method (Marubashi, 1997).

## 5. Problematic case 2: A large active region (AR12192) without halo CMEs, solar energetic particle events, and geomagnetic storms

AR12192 had its maximum area of 2,750 millionth of a solar disk according to the NOAA/Space Weather

Prediction Center (SWPC). This area is similar size with the maximum area of AR10486 of 2,610 millionth of a solar disk at the moment of the Halloween event in October 2003. Activities of AR10486 produced several very fast full halo CMEs and caused intense geomagnetic storms and solar energetic particle events as shown in Table 4.

However, activities of AR12192 produced almost no CME and did not cause solar energetic particle events and geomagnetic storms. AR12192 shows relatively simple magnetic configuration comparing with that of AR10486.

Figure 10 shows AR10486 (left panel) observed by the SOHO/Michelson Doppler Imager (MDI) and

AR12192 (right panel) observed by the SDO/Helioseismic and Magnetic Imager (HMI). Both active regions showed the modified Zurich sunspot group classification of Fkc and the Mt. Wilson magnetic classification of beta-gamma-delta and produced many X-class flares as shown in Table 4. Number of sunspot of AR10486 was 108. This is more than number of sunspot of 60 of AR12192. Figure 11 shows synoptic charts of the solar magnetic field of CR2009 (left panel) and CR2156 (right panel) produced by the WSO and rectangles show locations of AR10486 and AR12192, respectively. According to Figure 11, AR12192 had a large bipolar magnetic structure although AR10486 had a more complicated magnetic structure. This large bipolar magnetic structure of AR12192 seems to suppress occurrence of CMEs. This event remarks that a large active region with many intense flares does not always produce geomagnetic storms and solar energetic particle events.

## 6. Problematic case 3: A geomagnetic storm caused by a faint CME

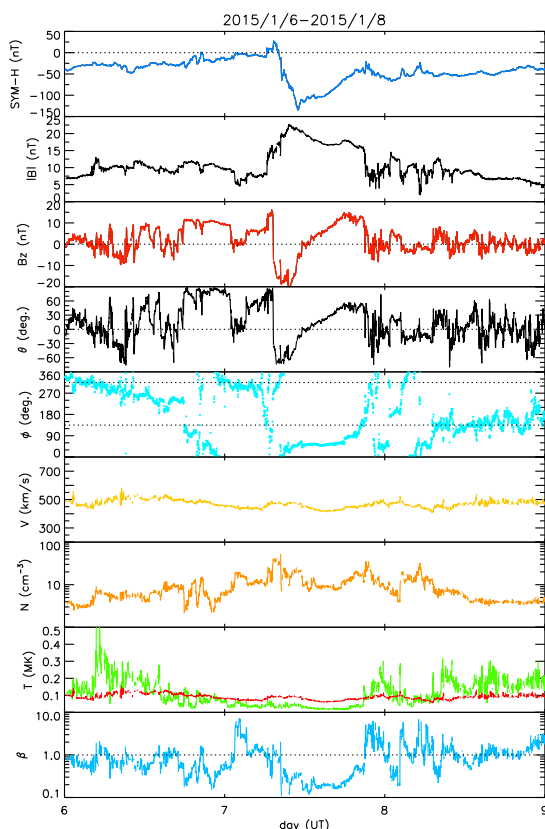


Figure 12. One-minute values of solar wind parameters near the earth with geomagnetic index, SYM-H between 6 and 8 in January 2015. Figure format is same as Figure 4.

A sudden commencement (SC) of geomagnetic storm occurred at 06:16 UT on 7 January 2015. The minimum Dst index of this geomagnetic storm was -99 nT. Occurrence of this storm was missed in our forecast because no obvious solar activity was recognized.

Figure 12 shows solar wind parameters between 6 and 8. According to Figure 12, solar wind speed of the

magnetic cloud associated with this storm is approximately 450 km/s and this speed is almost equal to the background solar wind speed. However, strong southward IMF continued for approximately three hours associated with the magnetic cloud. This caused the geomagnetic storm. Occurrence of solar source is expected on 3 January from the observed solar wind speed and timing of the SC. However, it is difficult to identify the solar source. This event remarks difficulty to estimate effect of a faint and slow CME without a remarkable counterpart on a solar disk.

## 7. Problematic case 4: Disagreement between observation and the Potential Field Source Surface (PFSS) Model on sector crossing

Figure 13 shows the coronal field map of CR2159 computed by the WSO based on the Potential Field Source Surface (PFSS) model. Blue, light shading shows the positive regions. The neutral line is black. According to Figure 13, the neutral line of the coronal field passed central meridian of the sun around 13 and 14 January. However, solar wind parameters shown in Figure 14 do not show a sector crossing associated with this neutral line. The away-sector continued between 8 and 20 according to Figure 14. This case suggests that sector change predicted by the coronal field map do not always agree with observation at 1 AU although we need to consider the modulation of IMF during propagation.

Coronal magnetic field maps calculated by the PFSS model are widely used for solar wind simulation models such as the WSA-Enlil model (Odstrcil et al., 2002; Odstrcil, 2003). This remarks that disagreement between solar wind observation near the earth and the PFSS model is a problem as an input of the present solar wind prediction models.

## 8. Summary

We studied the hit rate of space weather forecasts of the Japanese center and the several problematic events on the space weather forecasts during the analysis period.

The hit rates of the NICT space weather forecasts of solar flare activities and geomagnetic disturbances were calculated and they were compared with the hit rates of the forecasts using the persistence method. Both hit rates exceeded 50% during the analysis period and the forecasts of NICT were generally better than those by the persistence method. This is because we analyze flare history, magnetic classification, and area of each active region on the flare forecasts and estimate the effects of earth-directed halo CMEs and coronal holes on the geomagnetic disturbance forecasts.

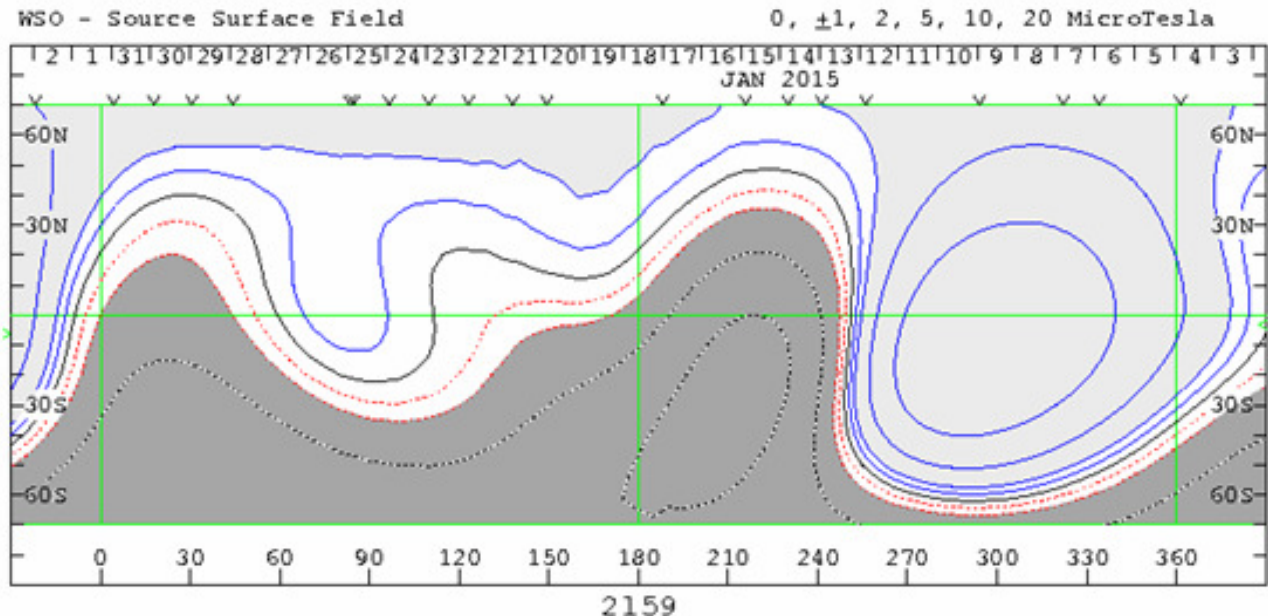


Figure 13. Coronal field map of Carrington Rotation 2159 computed by the WSO using the PFSS model. Blue, light shading shows the positive regions. The neutral line is black.

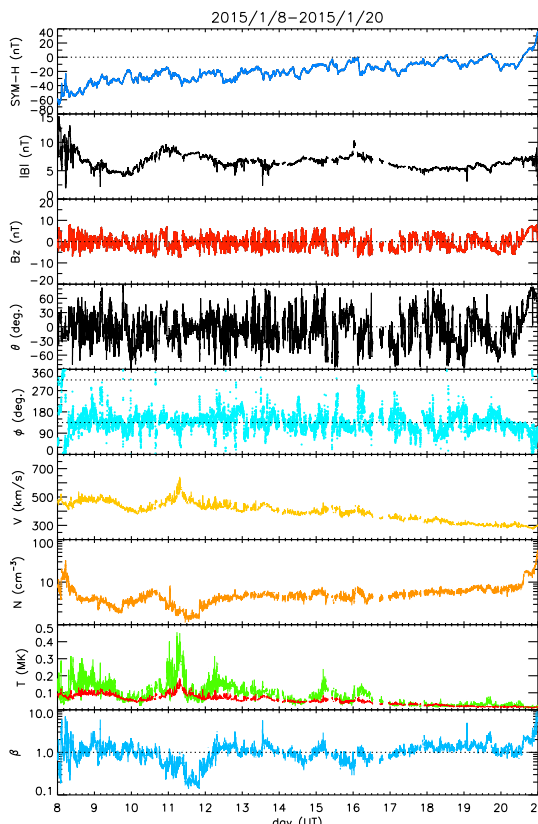


Figure 14. One-minute values of solar wind parameters near the earth with geomagnetic index, SYM-H between 8 and 20 in January 2015. Figure format is same as Figure 4.

Several problematic events on the space weather forecasts were analyzed using the events which occurred during the analysis period.

- (1) Different durations of southward IMF produced geomagnetic storms with different magnitudes such as the storm associated with the September 9, 2014 CME and the storm associated with the March 15, 2015 CME. We need a method to estimate southward IMF with long duration based on solar observations.
- (2) There are differences on productions of CMEs, solar energetic particle events, and geomagnetic storms according to magnetic configurations of active regions even though they show similar large size such as AR10486 and AR12192
- (3) The January 7, 2015 geomagnetic storm was caused by a faint CME. The speed of interplanetary CME was similar with back-ground solar wind speed. However, it carried strong southward IMF.
- (4) There is disagreement of timing of sector crossing between the in-situ observation at 1 AU and the prediction by the PFSS model in January 2015.

It is necessary for us to resolve those problems to improve our space weather forecasts. Discussion on the events in the STE workshop is important for this.

## Acknowledgements

We thank the NCEI, NOAA for the GOES flare lists, the Space Weather Prediction Center, NOAA for the active region reports, the Kakioka Magnetic Observatory, JMA for K indices, NASA for the SDO/AIA, SDO/HMI data, and OMNI data, ESA/NASA for the SOHO/MDI data, the World Data Center for Geomagnetism, Kyoto University for SYM-H, and the WSO for the solar magnetic field data. The STE workshop is supported by the STEL, Nagoya University.

This work was supported in part by JSPS Core-to-Core Program (B. Asia-Africa Science Platforms), Formation of Preliminary Center for Capacity Building for Space Weather Research and International Exchange Program of National Institute of Information and Communication Technology (NICT).

## References

- Gonzalez, W. D., Walter, D., and Tsurutani, B. T.: 1987, *Planet. Space Sci.*, 35, 1101, doi:10.1016/0032-0633(87)90015-8.
- Hyder, C. L.: 1967a, *Solar Phys.*, 2, 49, doi: 10.1007/BF00155892.
- Hyder, C. L.: 1967b, *Solar Phys.*, 2, 267, doi: 10.1007/BF00147842.
- Joselyn, J. A. and McIntosh, P. S.: 1981, *J. Geophys. Res.*, 86, 4555, doi: 10.1029/JA086iA06p04555.
- Lopez, R. E.: 1987, *J. Geophys. Res.*, 92, 11189, doi: 10.1029/JA092iA10p11189.
- Marubashi, K.: 1997 in N. Crooker, J. A. Joselyn and J. Feynman (eds.), *Coronal Mass Ejections*, *Geophys. Monogr. Ser.* Vol.99, AGU, Washington DC, p.147.
- Marubashi, K. and Lepping, R. P.: 2007, *Ann. Geophys.*, 25, 2453, doi: 10.5194/angeo-25-2453-2007.
- Odstrcil, D.: 2003, *Adv. Space Res.*, 32, 497, doi: 10.1016/S0273-1177(03)00332-6.
- Odstrcil, D., Linker, J. A., Lionello, R., Mikic, Z., Riley, P., Pizzo, V. J., and Luhmann, J. G.: 2002, *J. Geophys. Res.*, 107, SSH 14-1, doi 10.1029/2002JA009334.
- Watari, S.: 2008, *Adv. Space Res.*, 42, 1445, doi: 10.1016/j.asr.2007.02.029.